Electronic Supplementary Information

Constructing a Photo-Enzymatic Cascade Reaction and its *in situ* Monitoring: Enzymes Hierarchically Trapped in Titania Meso-Porous MOFs as a New Photosynthesis Platform

Junli Guo,[a] Lingling Yang,[a] Chenxi Zhao,[a] Zhida Gao,[a] Yan-Yan Song,*[a] and Patrik Schmuki*[b]

[a] College of Sciences, Northeastern University, Shenyang 110004, China

E-mail: yysong@mail.neu.edu.cn

[b] *Department of Materials Science, WW4-LKO, University of Erlangen-Nuremberg, 91058 Erlangen, Germany.*

E-mail: schmuki@ww.uni-erlangen.de

1. Chemicals and Reagents

Ti sheets (0.1 mm thickness, 99.6% purity) were purchased from Baosheng Hardware (Bao ji). 1,4-Dicarboxybenzene (BDC), 2-aminoterephthalic Acid (BDC-NH_2), cytochrome C (CytC), and titanium isopropoxide were purchased from Aladdin. 3,3′,5,5′-Tetramethylbenzidine (TMB), Acid orange 7 (AO7), N-(3-dimethylaminopropyl)-N′-ethyl-carbodiimide hydrochloride (EDC), and N-hydroxysuccinimide (NHS) were purchased from Sigma. Ammonium fluoride (NH_4F), ethylene glycol, N,N-dimethylformamide (DMF, 99.8%), methanol (CH_3OH), and other chemicals were purchased from Sinopharm Chemical Reagent and used as received without further purification. All aqueous solutions were prepared using Millipore Milli-Q water with a resistivity of 18.0 MΩ·cm.

2. Apparatus

UV-vis absorption spectra were recorded using a Perkin–Elmer spectrometer (Lambda 750S, USA). Morphology was characterized using a field-emission scanning electron microscope (Hitachi SU8000, Japan) and transmission electron microscope (TEM, JEM 2010, Japan). Crystal structures were identified by XRD acquired using an X'Pert XRD spectrometer (Philips, USA) using a CuKα X-ray source. FTIR spectroscopy was performed using a Nicolet 6700 instrument (Thermo Fisher, USA). N_2 adsorption–desorption isotherms were measured using a Micromeritics ASAP 2020 system. Prior to gas sorption measurements, 100 mg of as-formed samples was washed thoroughly with DMF and water to remove any remaining acetic acid, and then the sample was incubated in ethanol for 3 days, during which the solvent was decanted and freshly replenished three times every day. After that, the sample was dried under vacuum at 150 °C for 12 h to remove the remaining solvent, yielding a porous material. After ligand thermolysis, about 100 mg sample was treated under vacuum at 150 °C for 8 h before gas sorption experiment. In thermogravimetric analysis (TGA), 10 mg of the sample was heated using a TGA Q500 thermogravimetric analyzer from room temperature to 600 °C at a rate of 10 °C·min^{-1} under air flow of 20 mL· min^{-1}. A CHI660D electrochemical workstation (CH Instrument, USA) was used for all electrochemical tests equipped with two Ag/AgCl electrodes as the anode and cathode. Photocatalytic reactions were performed under the irradiation of a white LED (30 W, wavelength 400-600 nm).

3. Preparation of bulk R%-MIL-125-NH_2

The synthesis of R%-MIL-125-NH_2 is based on a reported method.[34,49] Briefly, after BDC, BDC-NH_2, and $Ti(OiPr)_4$ (1 mmol, 0.3 mL) were dissolved in 10 mL of a mixture of DMF and CH_3OH (V_{DMF}:V_{CH3OH} = 9:1), it was sonicated for 15 min at room temperature and then transferred to a 50 mL Teflon-lined autoclave. The sealed vessel was then heated at 150 °C for 24 h to obtain R%-MIL-125-NH_2. After cooling to room temperature, the synthesized product was washed with DMF and dried in a vacuum oven at room temperature.

4. Preparation of 30%-MIL-125-$NH_2$$(CytC)_{co}$/$TiO_2$M

CytC was grafted to the surface through EDC/NHS activation: 1.0 mL of 20 mg/mL solution of EDC and 10 mg/mL solution of NHS were added with 1.0 mg of CytC for 60 min to activate carboxylic group on CytC. Then 30%-MIL-125-NH_2/TiO_2M with –NH_2 groups were immersed in this solution for 12 h at room teperature. After grafting the modified grating was washed by ultrapure water and dried at room temperature.

5. Measurement of photocatalysis-generated H_2O_2

UV-Vis spectra were used to detect H_2O_2 produced by hpMIL-125/TiO_2M and Au@hpMIL-125/TiO_2M. Briefly, 3 mg Au@hpMIL-125/TiO_2M was dipped in 1 mL H_2O and then exposed to visible-light irradiation (30 W white LED light). After irradiation for a certain period, 1.5 mM ABTS and 0.1 mg/mL HRP were added. After incubating the solution at 37 °C for 20 min in dark, the absorption spectra of ABTS at 734 nm were recorded using a Perkin–Elmer spectrometer.

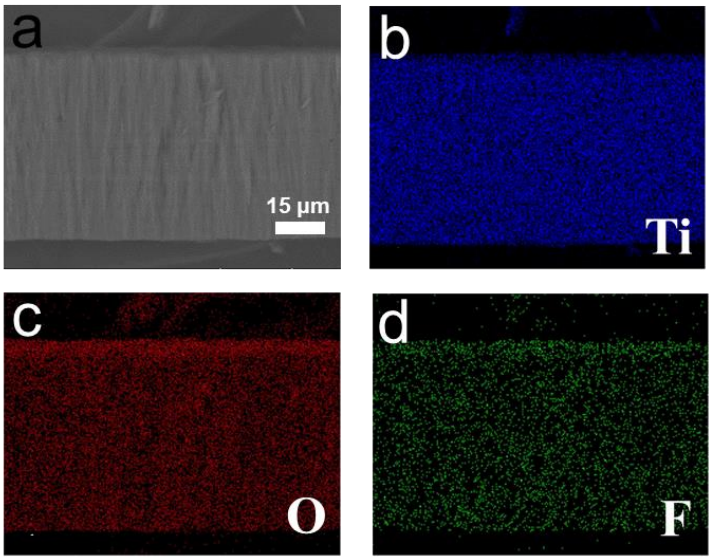

Fig. S1 (a) SEM cross-sectional image of amorphous TiO_2M. EDS-SEM cross-sectional mapping for different elements of amorphous TiO_2M: (b) Ti, (c) O, (d) F.

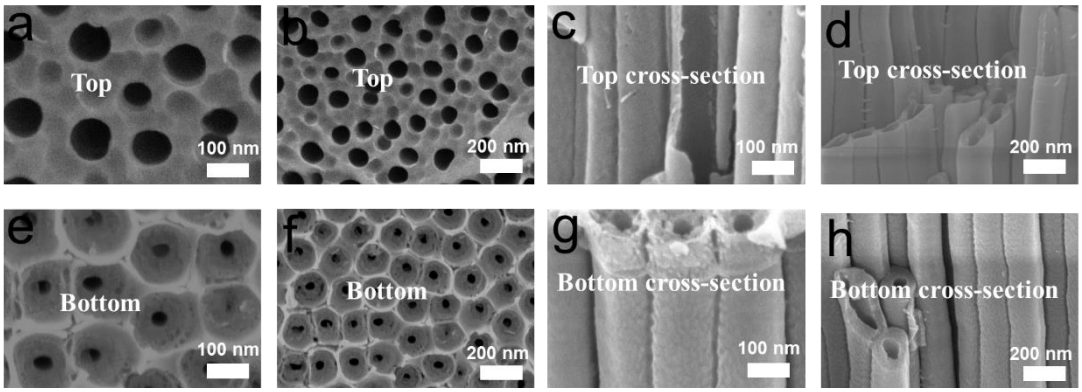

Fig. S2 (a) SEM images of TiO_2M treatment in a 50 mL Teflon-lined autoclave containing 200 µL HCl (0.1 M), 9 mL DMF and 1mL CH_3OH at 150 ^oC for 12 h ((a, b) top view, (c, d) top cross-section, (e, f) bottom view, (g, h) bottom cross-section).

In Fig. S2, the hydrothermal treatment in organic solution without ligands keeps the architecture of TiO_2 nanochannel wall. No crystallite can be found on the wall. Therefore, the plate-like nanocrystals observed in our experiment can be ascribed to the metal-organic framework formed by the coordination of the ligands (BDC or BDC-NH_2) and Ti^{4+}.

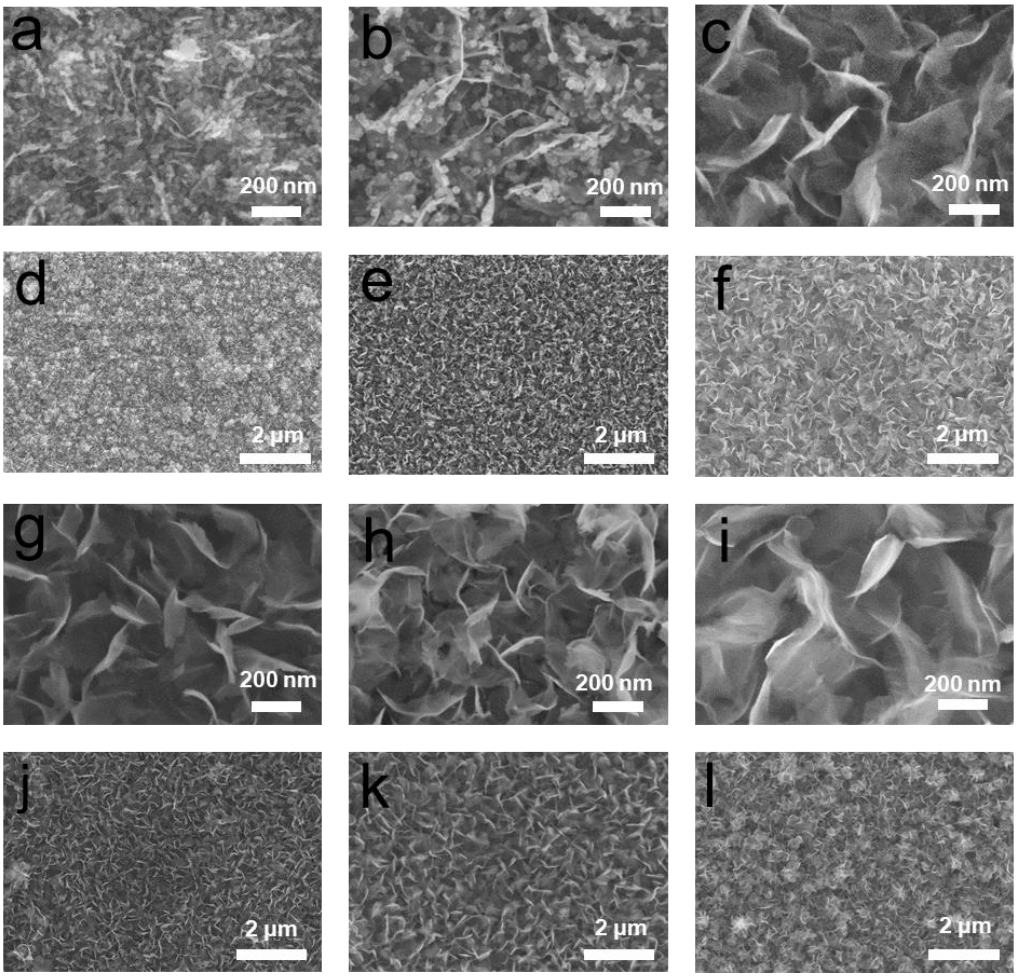

Fig. S3 SEM images of (a, d) MIL-125/TiO_2M, (b, e) 10%-MIL-125-NH_2/TiO_2M, (c, f) 20%-MIL-125-NH_2/TiO_2M, (g, j) 30%-MIL-125-NH_2/TiO_2M, (h, k) 40%-MIL-125-NH_2/TiO_2M, (i, l) 50%-MIL-125-NH_2/TiO_2M.

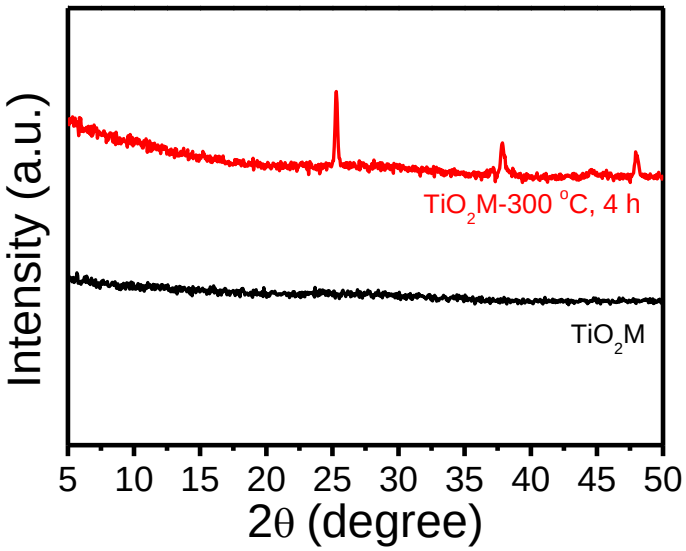

Fig. S4 XRD patterns of TiO_2M treatment in a 50 mL Teflon-lined autoclave containing 200 µL HCl (0.1 M), 9 mL DMF and 1mL CH_3OH at 150 ^oC for 12 h (black line) and TiO_2M annealed at 300 ^oC for 4 h (red line).

As demonstrated by XRD results, TiO_2M is still amorphous (black line) after undergoing the hydrothermal treatment in the absence of ligands.

The annealing treatment at 300 ^oC for 4 h transfers the amorphous TiO_2 to anatase crystalline (red line).

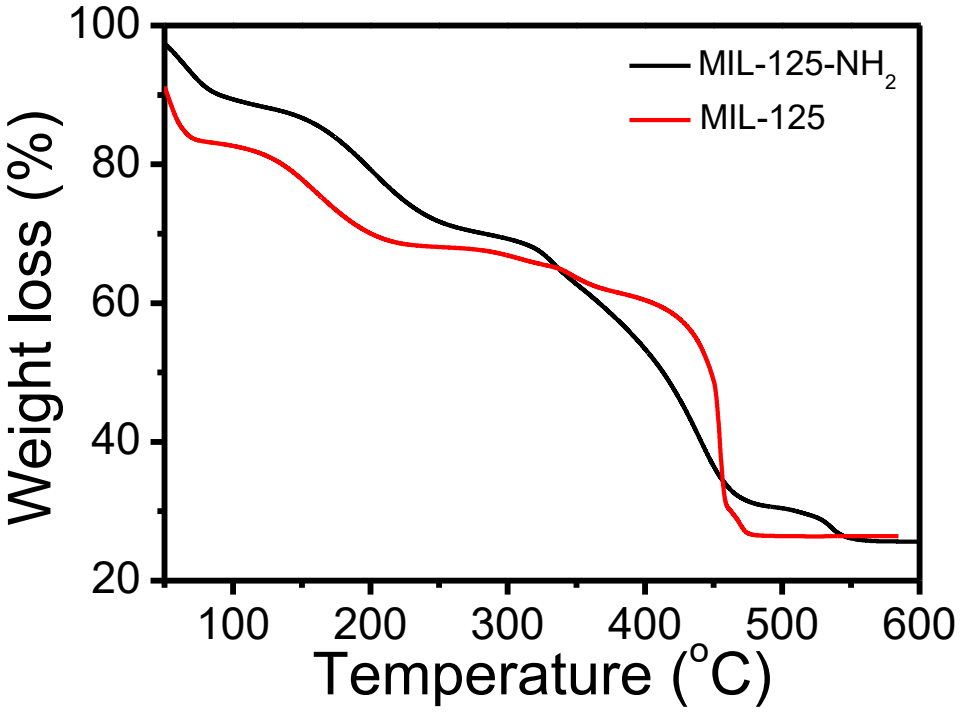

Fig. S5 Thermogravimetric analyses (TGA) of MIL-125 and MIL-125-NH_2.

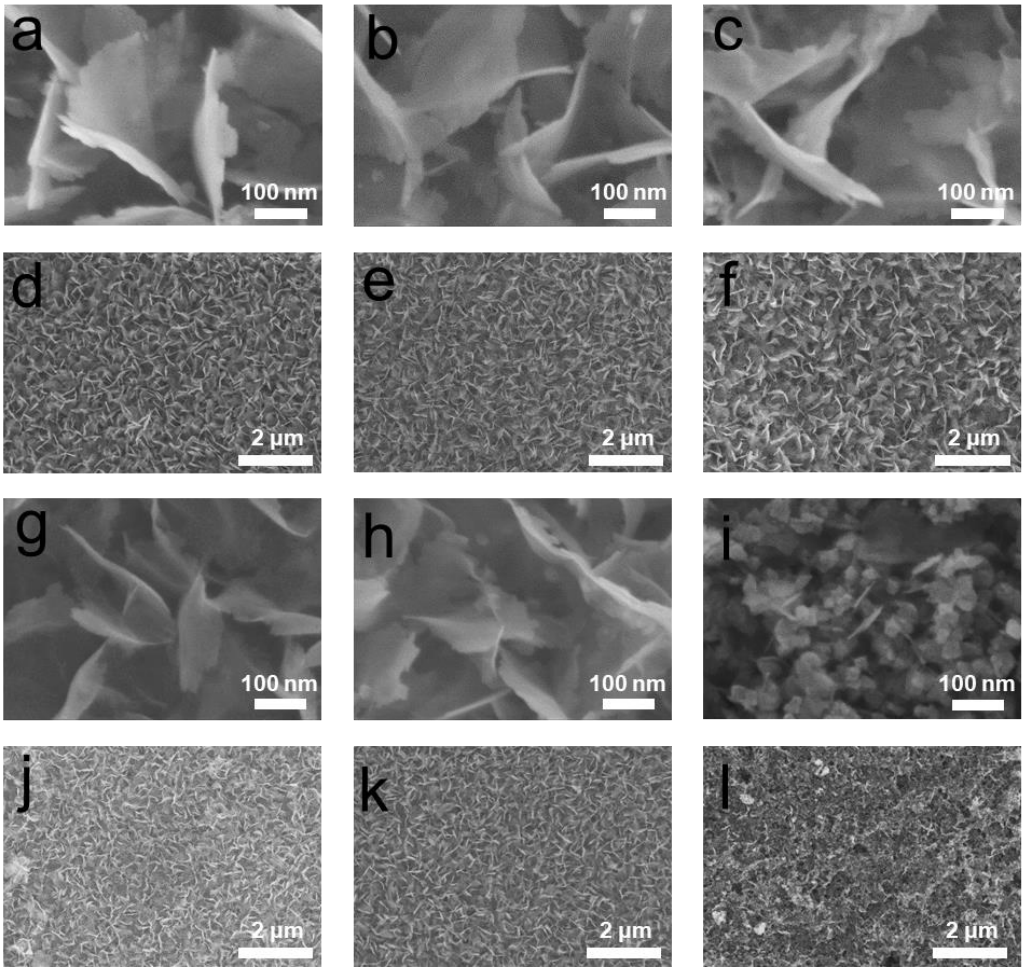

Fig. S6 SEM of 30%-MIL-125-NH_2/TiO_2M annealed for (a, d) 0.5 h, (b, e) 1 h, (c, f) 2 h, (g, j) 4 h, (h, k) 6 h and (i, l) 8 h at 300 °C in air.

SEM images show that the plate-like MOFs on the membrane surface and on the channel walls maintain their typical structure after a 0.5-4 h thermolysis treatment (Fig. S6). However, a further increase in thermolysis time to 6 h (Fig. S6h, k) or 8 h (Fig. S6i, l), leads to a collapse of the MOF nanocrystals.

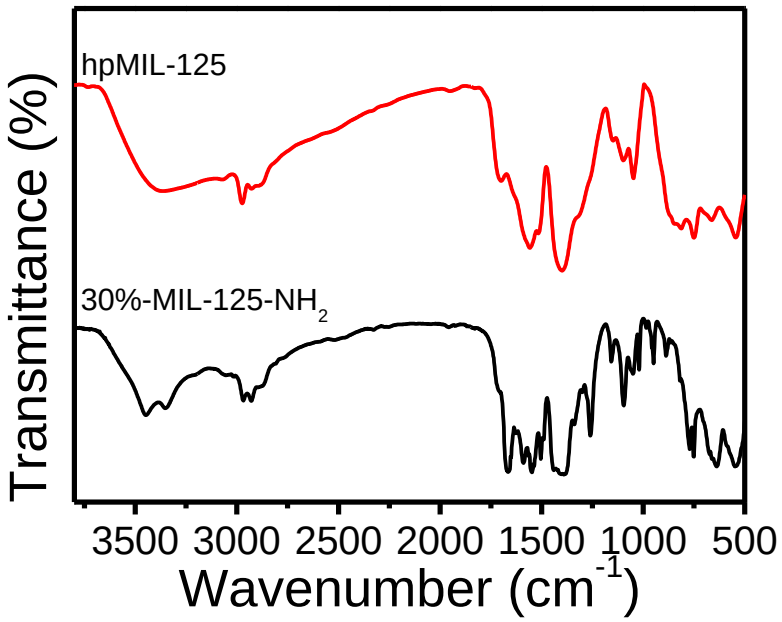

Fig. S7 FTIR of 30%-MIL-125-NH_2 before and after annealing at 300 °C for 4 h in air.

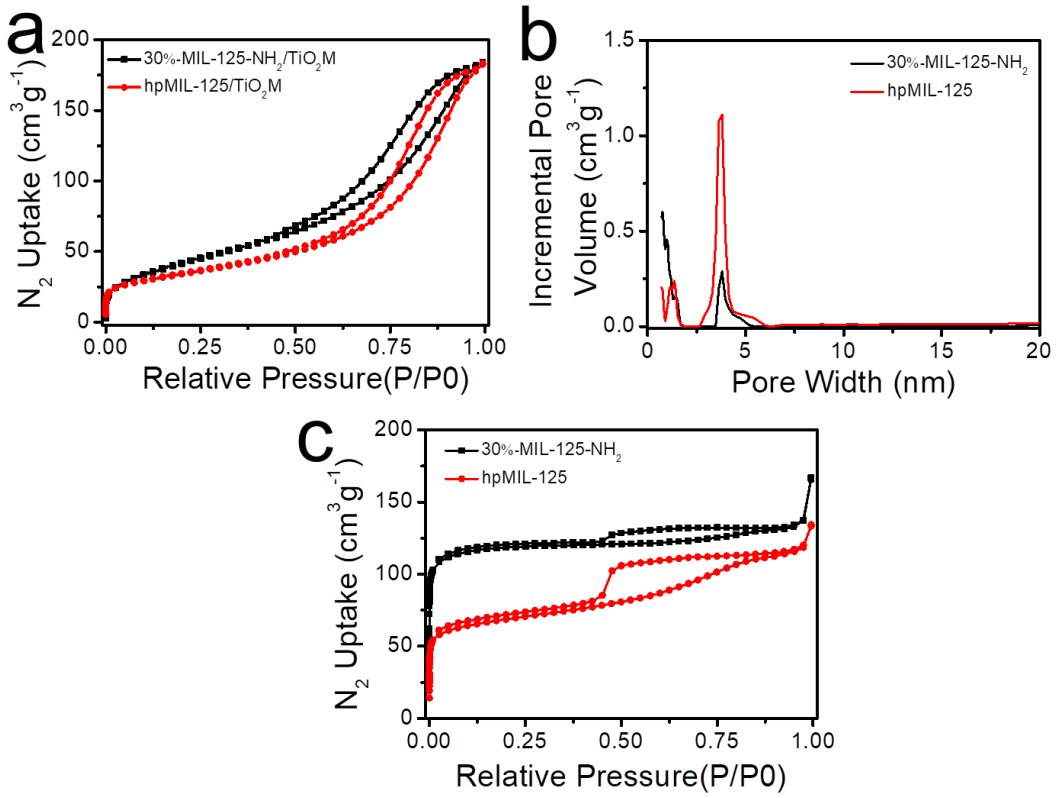

Fig. S8 (a) N_2 sorption isotherms of 30%-MIL-125-NH_2/TiO_2M before and after linker thermolysis. (b) Pore size distributions of 30%-MIL-125-NH_2 before and after thermolysis treatment. (c) N_2 sorption isotherms of 30%-MIL-125-NH_2 before and after linker thermolysis.

Both 30%-MIL-125-NH_2 and hpMIL-125 (Fig. S8c) exhibit similar sorption isotherms containing a combination of type I and IV sorption curves. The high adsorption amount of N_2 occurring at a low relative pressure demonstrates the presence of micropores.[1-3] Meanwhile, the hysteresis at a relative pressure of ~0.5, associating with capillary condensation of N_2 within mesopores, demonstrates the presence of a mesostructure in 30%-MIL-125-NH_2 and hpMIL-125 samples.[4,5] The ratio of meso- to micropore volume on hpMIL-125 proportionally increases as indicated by the increased intensity at a pore size of ~4.5 nm (Fig. S8b). The mesopores in 30%-MIL-125-NH_2/TiO_2M can be explained by the presence of nonrigid aggregates of plate-like nanocrystals.[6] The specific surface area of 30%-MIL-125-NH_2 is 467 $m^2 g^{-1}$, and it decreases to 255 $m^2 g^{-1}$ after the thermolysis treatment.

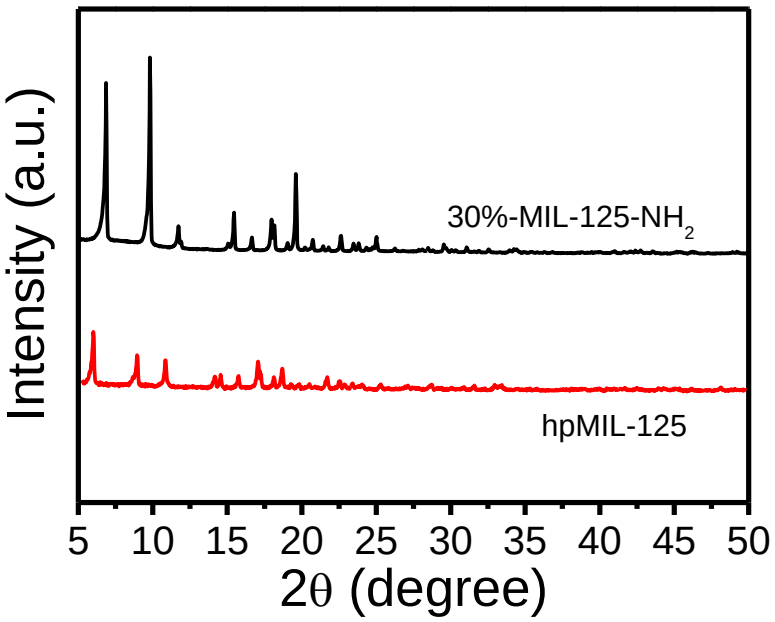

Fig. S9 XRD patterns of 30%-MIL-125-NH_2 before and after annealing at 300 °C in air for 4 h.

Table S1 Zeta potentials

Sample	Zeta potential (mV)
TiO_2M	−11.1
30%-MIL-125-NH_2/TiO_2M	−24.8
hpMIL-125/TiO_2M	−4.06
Au@hpMIL-125/TiO_2M	−28.6
Au@hpMIL-125(CytC)/TiO_2M	−17.7

The as-formed TiO_2M has a negative surface charge (zeta potential, −11.1 mV). Owing to the presence of carboxyl groups on BDC and BDC-NH_2, the zeta potential negatively shifts to −24.8 mV by forming 30%-MIL-125-NH_2/TiO_2M. Upon the removal of MIL-125-NH_2 by thermolysis, the hpMIL-125/TiO_2M provides fewer negative charges (zeta potential, −4.08 mV).

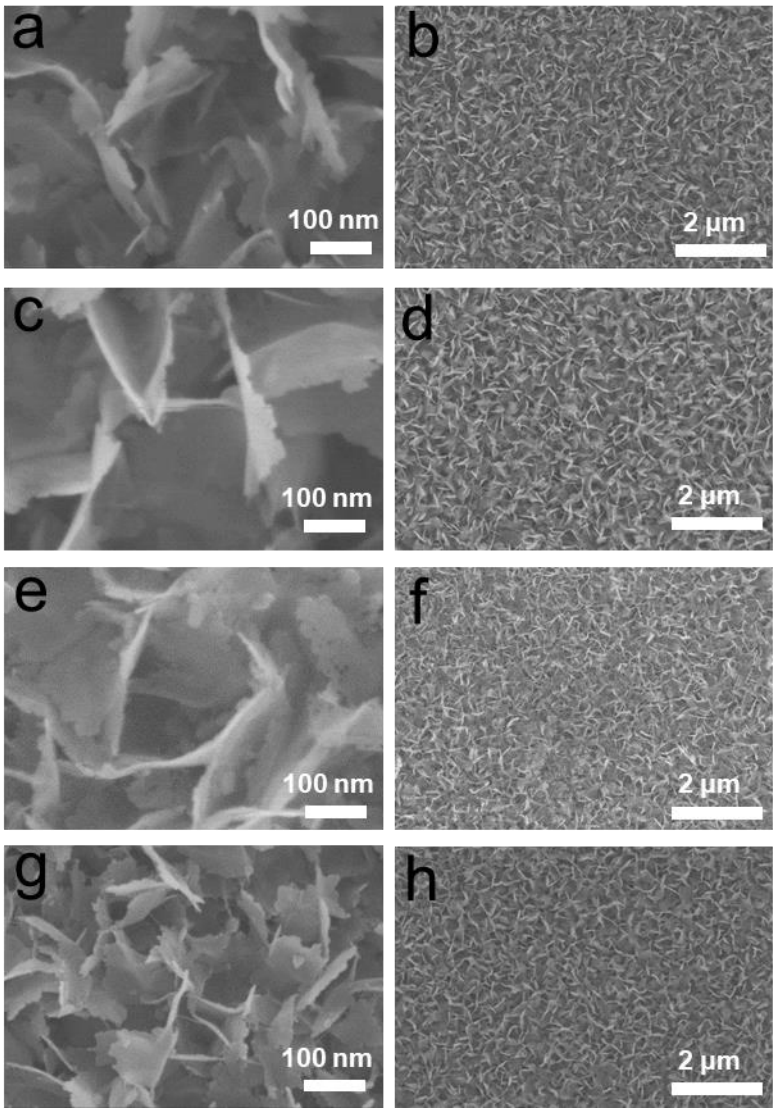

Fig. S10 SEM of hpMIL-125/TiO_2M soaked in water for different periods (a, b) 4 h, (c, d) 24 h, (e, f) 4 d, (g, h) 10 d.

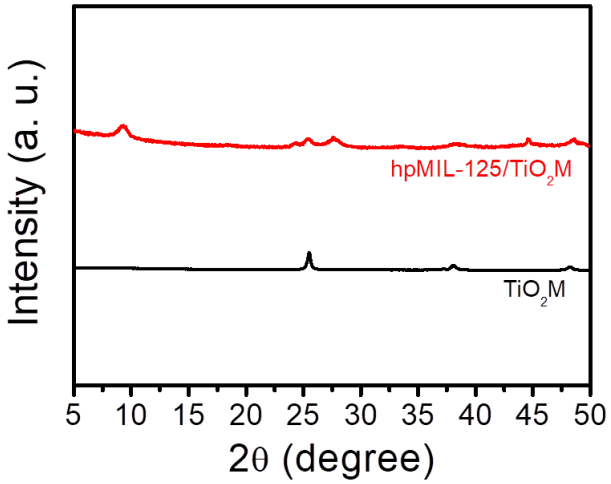

Fig. S11 XRD patterns of anatase TiO_2M (annealed at 300 °C for 4h) and as-proposed hpMIL-125/TiO_2M after soaking in DI water at room temperature for 10 days.

Compared with the XRD patterns of freshly prepared anatase TiO_2M (Fig. S4) and hpMIL-125/TiO_2M (Fig. 1l), it can be concluded that these membranes maintain their crystal structures after the long-time soaking in water.

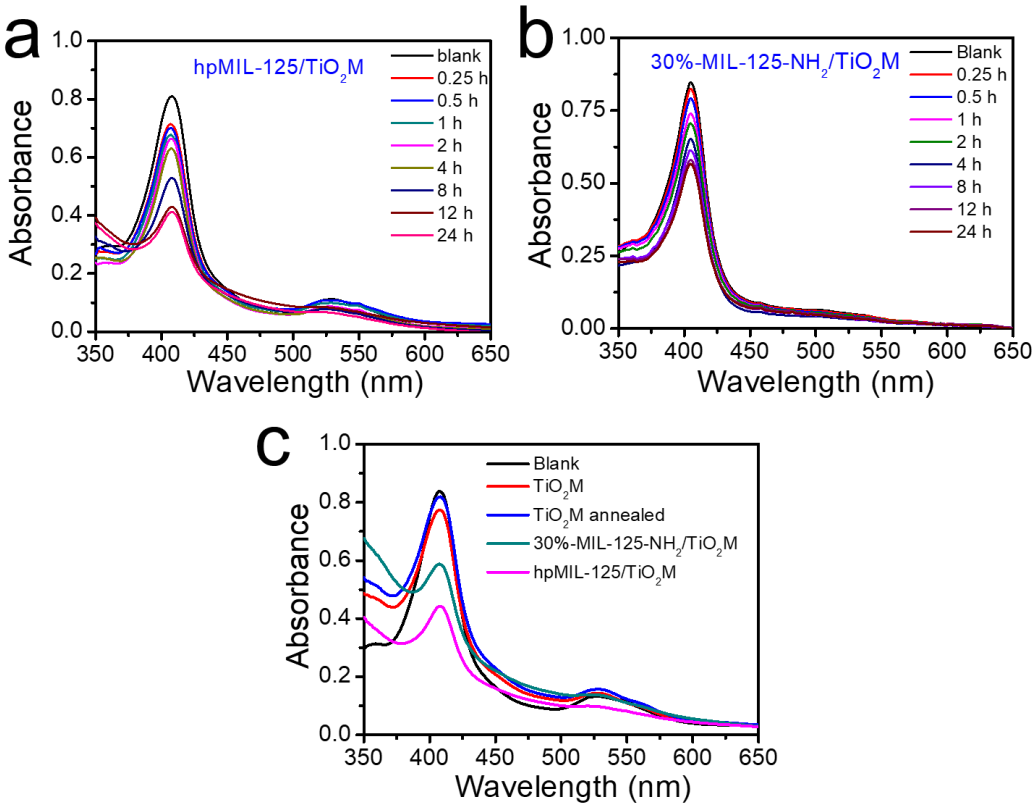

Fig. S12 UV-Vis absorption spectra of CytC in the remaining solution after incubation treatment with 3 mg (a) hpMIL-125/TiO_2M and (b) 30%-MIL-125-NH_2/TiO_2M in different time. (c) UV-Vis adsorption spectra of CytC in the remaining solution after incubation for 12 h with different samples.

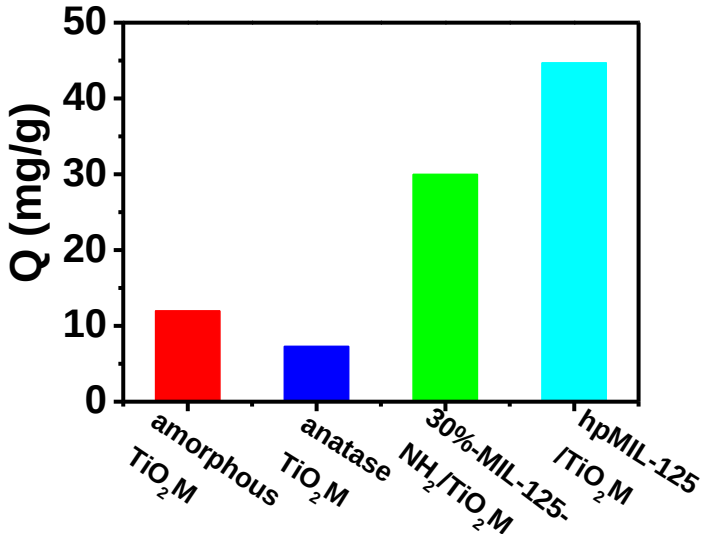

Fig. S13 Adsorption capacity of CytC on amorphous TiO_2M, anatase TiO_2M, 30%-MIL-125-NH_2/TiO_2M, and hpMIL-125/TiO_2M.

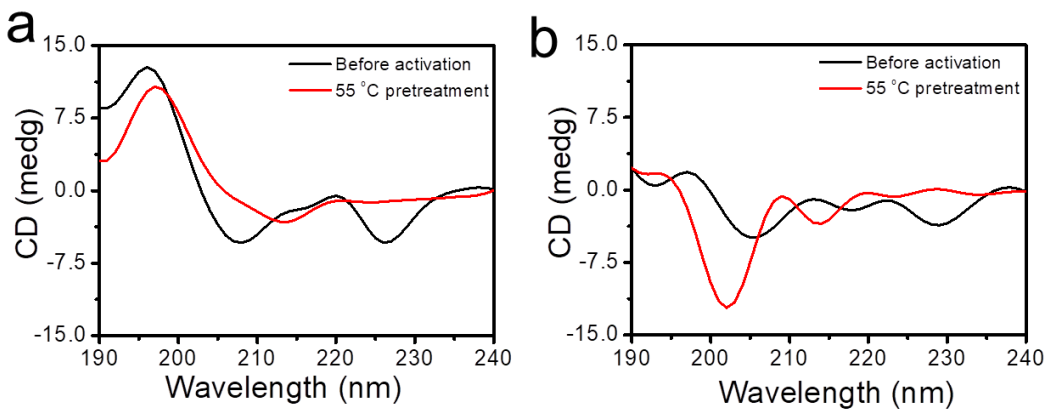

Fig. S14 CD spectrum of a) 30%-MIL-125-NH_2(CytC)/TiO_2M and b) 30%-MIL-125-$NH_2$$(CytC)_{co}$/$TiO_2$M before and after incubating at 55 °C for 2 h.

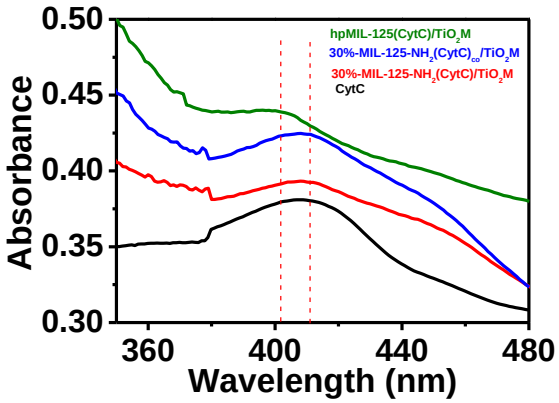

Fig. S15. UV−vis diffuse reflectance spectra of CytC (CytC mixed with $BaSO_4$ to press tablet), 30%-MIL-125-NH_2(CytC)/TiO_2M, 30%-MIL-125-NH_2(CytC)$_{co}$/TiO_2M and hpMIL-125/TiO_2M. A high-purity $BaSO_4$ was used as the background.

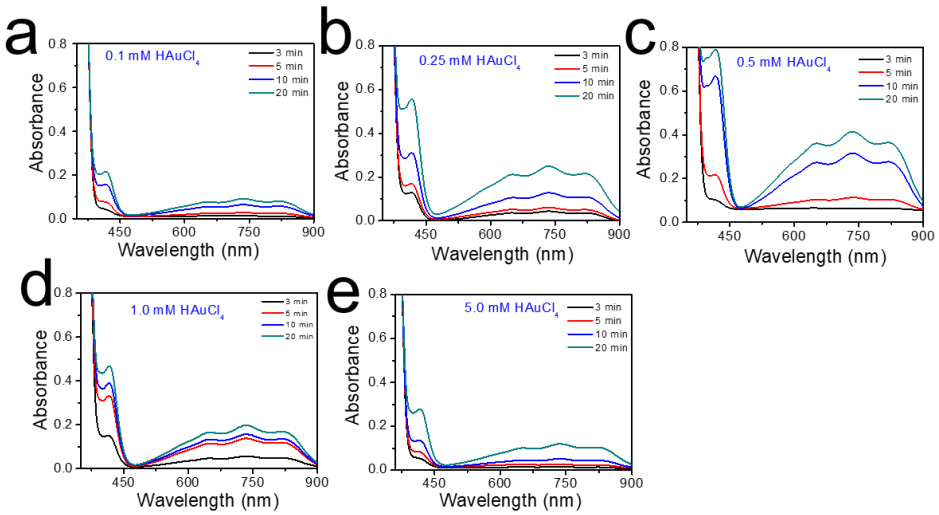

Fig. S16 Effect of Au loading amount on H_2O_2 generation. UV-Vis spectra of APTS in the presence of HRP and Au@hpMIL-125/TiO_2M under irradition for different time. The concentrations of $HAuCl_4$ are (a) 0.1 mM, (b) 0.25 mM, (c) 0.5 mM, (d) 1 mM, and (e) 5 mM.

The as-prepared Au@hpMIL-125/TiO_2M (3 mg in 1 mL H_2O) was irradiated with a 30 W white LED light in a quartz cuvette. After irradiation, 1.5 mM ABTS and 0.1 mg/mL HRP were added and then incubated at 37 °C for 20 min. The absorption spectra of ABTS at 734 nm were recorded using a spectrometer.

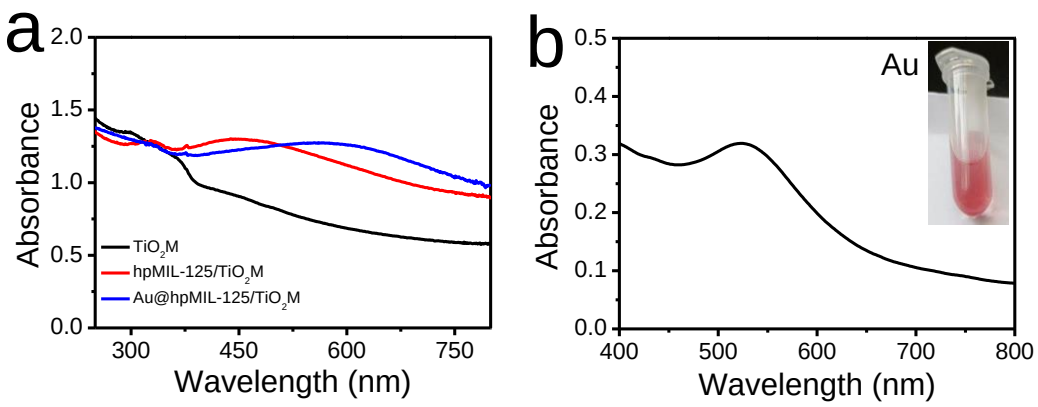

Fig. S17 (a) UV/visible diffuse reflectance spectra of TiO_2M, hpMIL-125/TiO_2M, and Au@hpMIL-125/TiO_2M. (b) UV-Vis absorption spectra of Au NPs peeled from Au@hpMIL-125/TiO_2M. Inset image: the corresponding digital photographs of the Au NPs solution.

Figure S16 b shows the UV-Vis adsorption spectrum of Au NPs which are achieved by immersing the Au@hpMIL-125/TiO_2M sample in a 5% HF solution at 60 ^{o}C for 2 h to resolve hpMIL-125/TiO_2M. The UV-vis absorption spectrum (Fig. S16b) and digital image (inset of Fig. S16b) verify the typical SPR characters of the AuNPs on the sample.

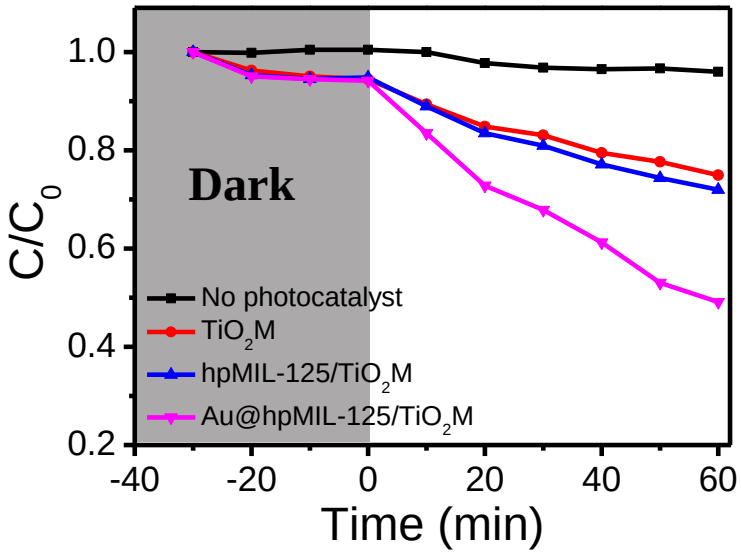

Fig. S18 Photocatalytic degradation of AO7 in the presence of different photocatalysts. AO7: 25 μM; light source: 30W LED (400-600 nm).

Owing to the wide band-gap of TiO_2 and ML-125, bare TiO_2M and hpMIL-125/TiO_2M samples only present poor photocatalytic activities in the visible-light irradiation (400-600 nm LED). After AuNPs grafting, the resulted Au@hpMIL-125/TiO_2M sample shows an enhanced photocatalytic activity in the visible-light range. This improvement can be attributed to the SPR of AuNPs, by which the hot electrons generated by the excited SPR state are injected into the CB of TiO_2.

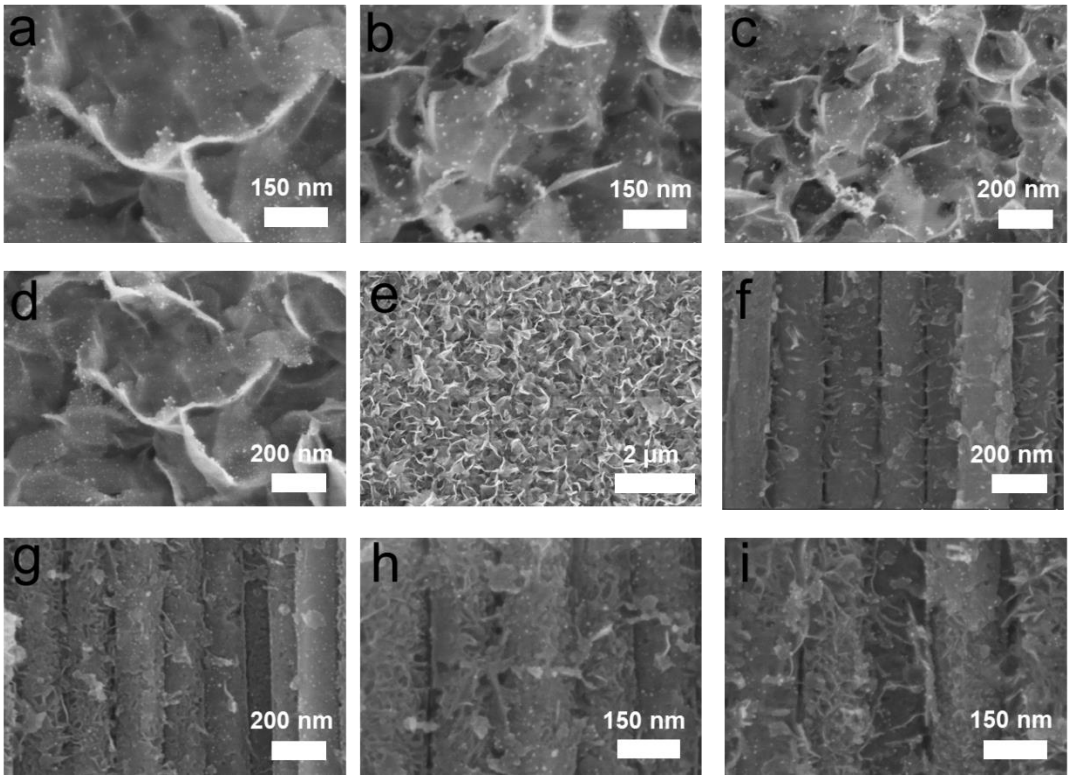

Fig. S19 SEM images of Au NP-modified hpMIL-125/TiO_2M.

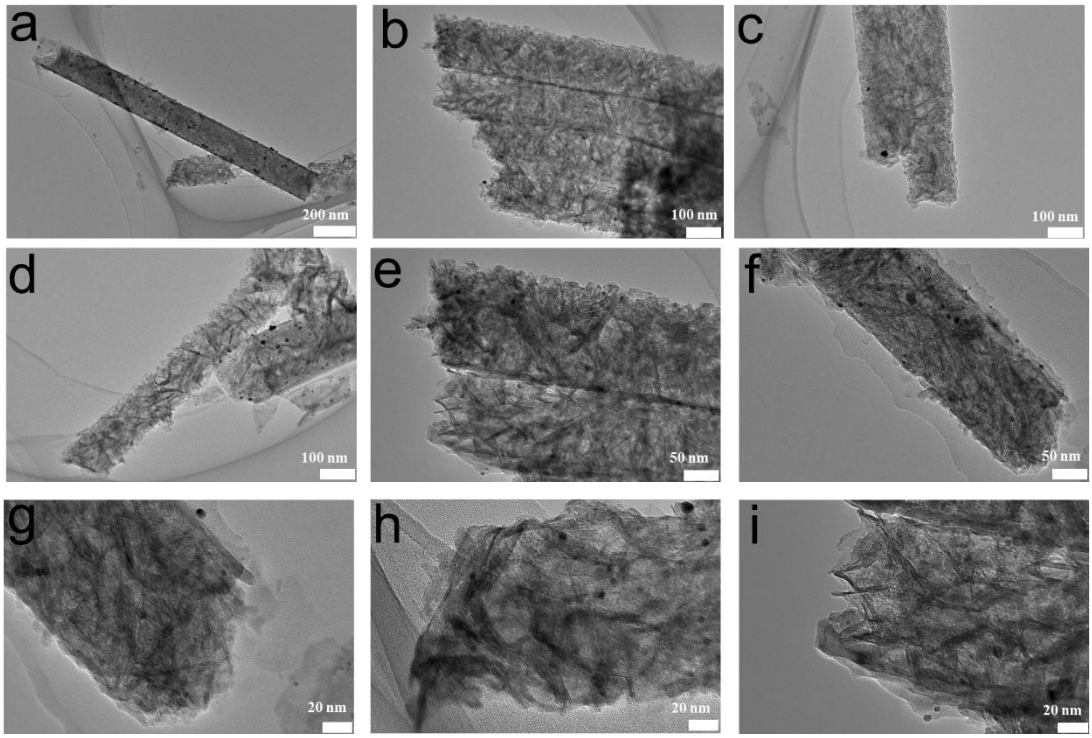

Fig. S20 TEM images of Au NP-modified hpMIL-125/TiO_2M.

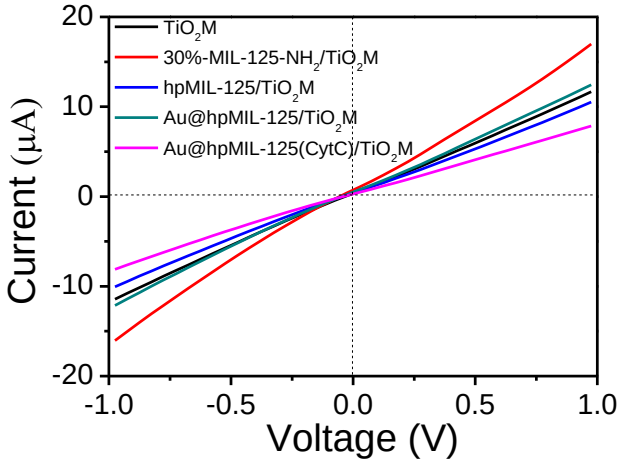

Fig. S21 *I-V* properties of bare TiO_2M (black line), 30%-MIL-125-NH_2 (red line), annealed at 300 °C for 4 h (blue line), modified with Au NPs (green line), and encapsulation of CytC (purple line).

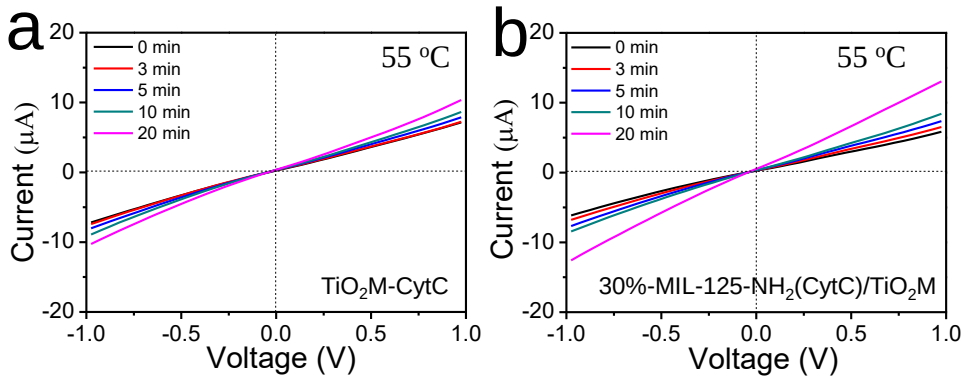

Fig. S22 *I-V* properties of (a) TiO_2M-CytC and (b) 30%-MIL-125-NH_2(CytC)/TiO_2M in 1.0 mM KCl after irradiating for different periods by LED.

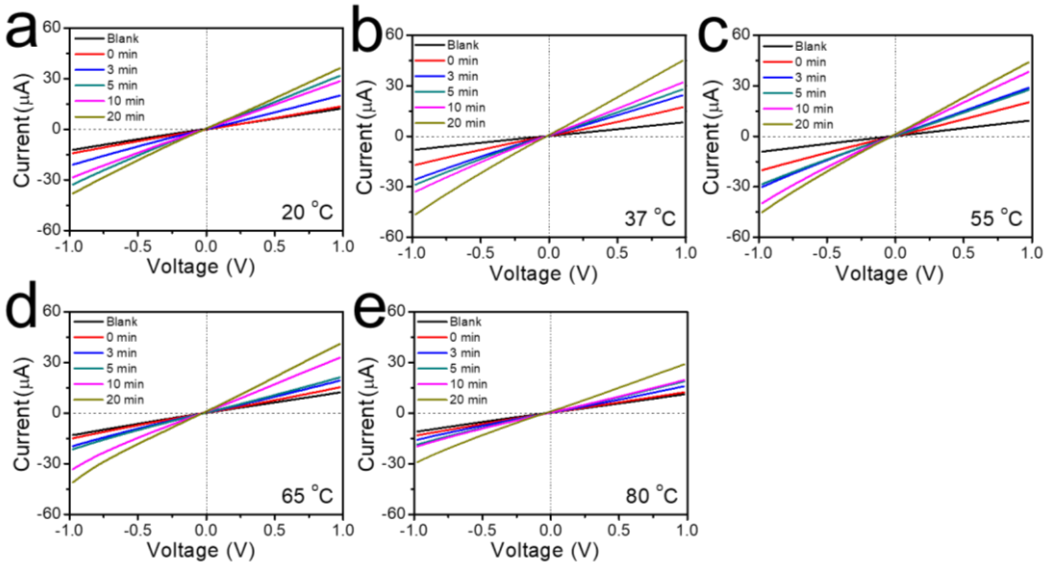

Fig. S23 *I-V* properties of freshly prepared Au@hpMIL-125(CytC)/TiO_2M samples with different irradiation time. Before the ionic current measurements, the samples were first pretreated at different temperatures for 2 h: (a) 20 °C, (b) 37 °C, (c) 55 °C, (d) 65 °C, (e) 80 °C.

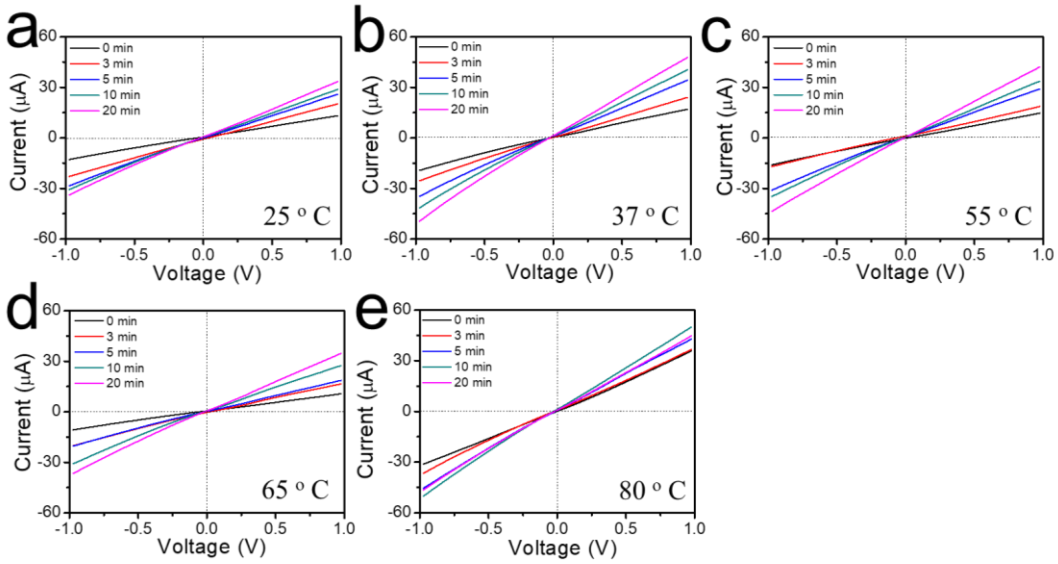

Fig. S24 *I-V* properties of Au@hpMIL-125(CytC)/TiO_2M samples with different irradiation time after storage for 7 days at room temperature. Before the ionic current measurements, the samples were first pretreated at different temperatures for 2 h: (a) 20 °C, (b) 37 °C, (c) 55 °C, (d) 65 °C, (e) 80 °C.

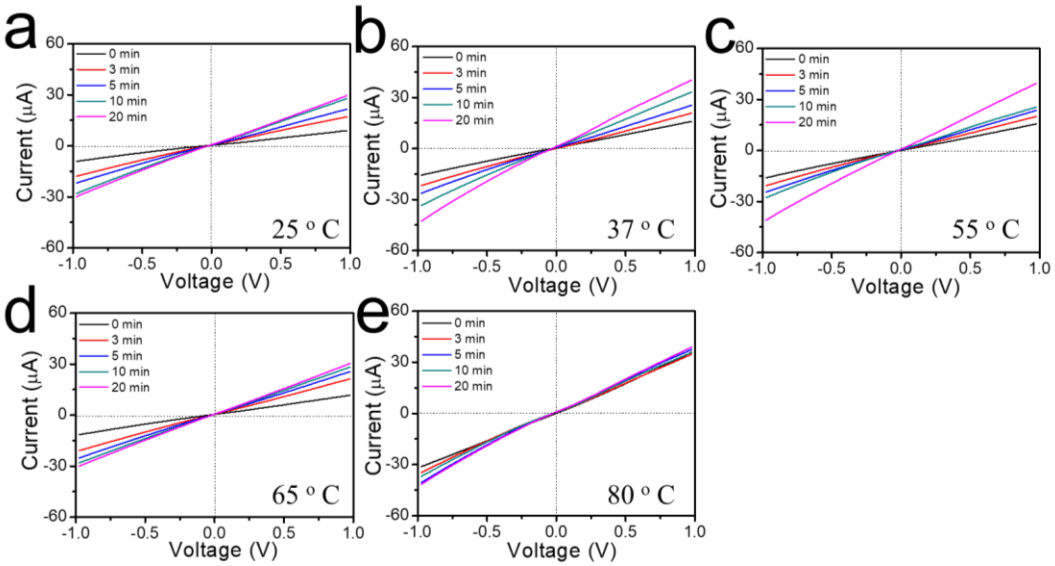

Fig. S25 *I-V* properties of Au@hpMIL-125(CytC)/TiO_2M samples with different irradiation time after storage for 21 days at room temperature. Before the ionic current measurements, the samples were first pretreated at different temperatures for 2 h: (a) 20 °C, (b) 37 °C, (c) 55 °C, (d) 65 °C, (e) 80 °C.

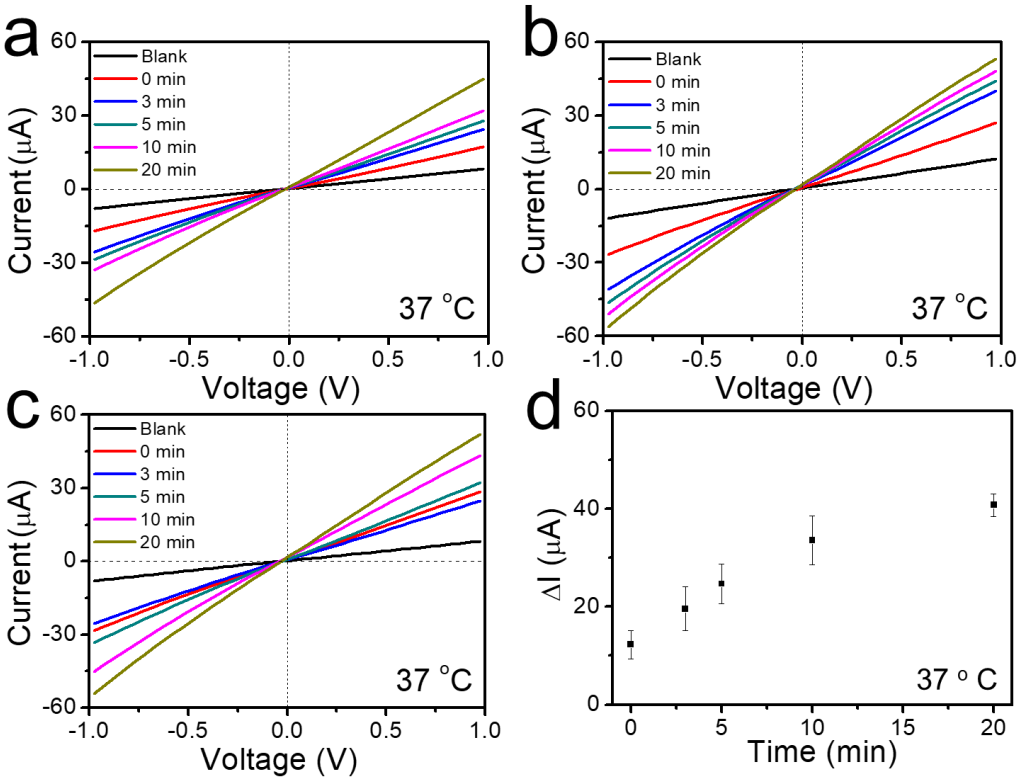

Fig. S26 (a, b, c) Parallel *I-V* profiles of three different Au@hpMIL-125(CytC)/TiO_2M samples for constructing a cascade reaction. (d) Corresponding calibration plots (the change in current at +1.0 V) of the proposed sensing device. All the samples were activated at 37 °C for 2 h.

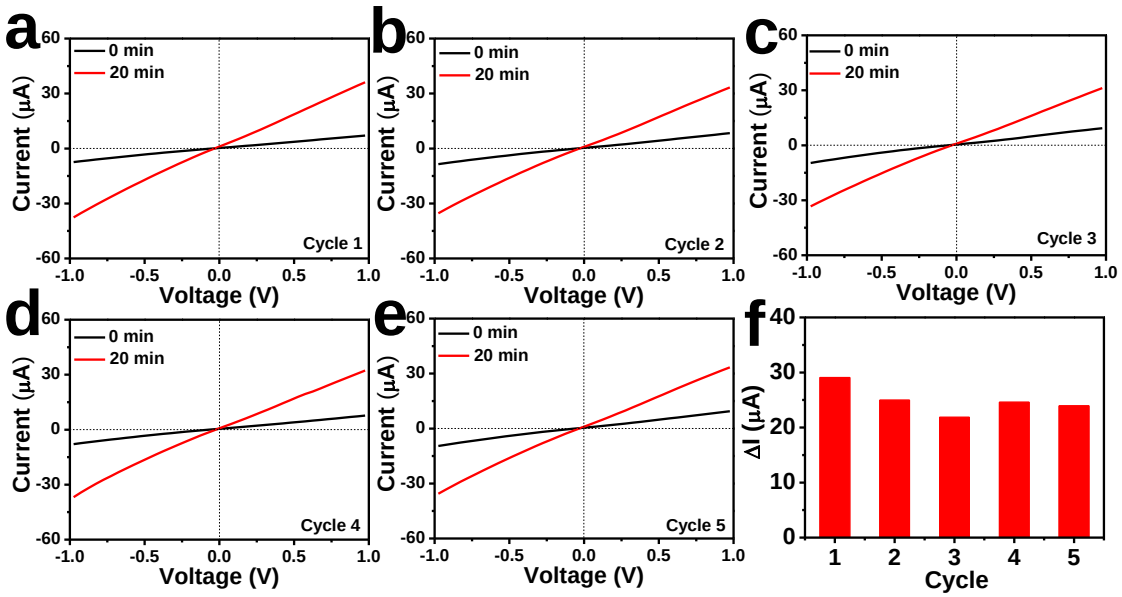

Fig. S27. (a-e) *I-V* properties of Au@hpMIL-125(CytC)/TiO_2M at different cycles. (f) ΔI values of Au@hpMIL-125(CytC)/TiO_2M at +1.0 V before and after cascade reactions in different application cycles. The sample was activated at 55 ^{o}C for 2 h before *I-V* property measurements.

References

1 G. R. Cai and H. L. Jiang, *Angew. Chem. Int. Ed*., 2017, **56**, 563−567.

(2) M. R. DeStefano, T. Islamoglu, S. J. Garibay, J. T. Hupp and O. K. Farha, *Chem. Mater.,* 2017, **29**, 1357−1361.

(3) R. X. Chen, J. G. Yu and W. Xiao, *J. Mater. Chem. A,* 2013, **1**, 11682.

(4) Z. Wang, S. G. Hu, J. Yang, A. J. Liang, Y. S. Li, Q. X. Zhuang and J. L. Gu, *Adv. Funct. Mater.,* 2018, **28**, 1707356.

(5) L. B. Sun, J.-R. Li, J. H. Park and H.-C. Zhou, *J. Am. Chem. Soc.,* 2012, **134**, 126−129.

(6) M. Thommes, *Chemie Ingenieur Technik*, 2010, **7**, 1059−1073.